IEEE Access
Multidisciplinary | Rapid Review | Open Access Journal

IEEE POWER & ENERGY SOCIETY SECTION

Received 27 October 2023, accepted 10 November 2023, date of publication 14 November 2023,
date of current version 17 November 2023.

Digital Object Identifier 10.1109/ACCESS.2023.3332662

RESEARCH ARTICLE

An Efficient and Reliable Electric Power Transmission Network Topology Processing

DULIP MADURASINGHE, (Graduate Student Member, IEEE), AND GANESH KUMAR VENAYAGAMOORTHY, (Fellow, IEEE)

Real-Time Power and Intelligent Systems Laboratory, Holcombe Department of Electrical and Computer Engineering, Clemson University, Clemson, SC 29634, USA

Corresponding author: Dulip Madurasinghe (dtmadurasinghe@ieee.org)

This work was supported in part by the National Science Foundation (NSF), USA, under Grant CNS 2131070, Grant ECCS 2234032, and Grant CNS 2318612; and in part by the Duke Energy Distinguished Professorship Endowment Fund.

ABSTRACT The modern bulk power system operation is complex and dynamic, with rapidly increasing inverter-based resources and active distribution systems. Therefore, high-speed monitoring is required to operate the power system reliably and efficiently. Transmission network topology processing (TNTP) is vital in power system control. Today's TNTP is based on supervisory control and data acquisition (SCADA) system monitoring of relay signals (SMRS). Due to the slow data communication rate, SMRS cannot efficiently support the modern bulk power system's energy management system (EMS) functions. In this study, a physics-based hierarchical TNTP (H-TNTP) approach based solely on node voltages and branch currents measurements is proposed utilizing artificial intelligence algorithms. H-TNTP includes the identification of substation configuration. The reliability of the H-TNTP is guaranteed by the design with inherent verification. If required, H-TNTP is capable of operating concurrently with the TNTP-SMRS. A power system with solar photovoltaic (PV) plants is utilized as a test system to illustrate the proposed H-TNTP approach. Results indicate that H-TNTP is fast with synchrophasor measurements. Furthermore, to demonstrate the application of the reliable and fast TNTP approach in EMSs, fast automatic generation control (AGC) during contingencies is studied. Typical results show that fast reconfiguration of AGC modes and dispatch factors leads to better frequency regulation.

INDEX TERMS Artificial intelligence, reconfigurable automatic generation control, substation configuration identification, transmission network topology processor.

NOMENCLATURE

AGC	Automatic generation control.
AI	Artificial intelligence.
AS	Area separation.
B_1	Input layer bias.
B_2	Hidden layer bias.
BBM	Bus-branch mode.
BCM	Branch connectivity matrix.
BHA	Breaker and half arrangement.
CI	Configuration identification.
CIM	Common information model.
DBSBA	Double bus single breaker arrangement.
DBDBA	Double bus double breaker arrangement.
DER	Distributed energy resources.
DR	Demand response.
ECC	Energy control center.
EMS	Energy management system.
EV	Electrical vehicle.
FA	Functional arrangement.
H-TNTP	Hierarchical transmission network topology processing.
H-TNTP-PMU	Synchrophasor based hierarchical transmission network topology processing.
ICCP	Inter-control center communications protocol.
LDM	Logical decision-making.
LSE	Linear state estimator.

The associate editor coordinating the review of this manuscript and approving it for publication was Cuo Zhang.

MTBA	Main and transfer bus arrangement.
NBM	Node-branch mode.
NCM	Node connectivity matrix.
NLP	Network-level processing.
NN	Neural network.
PiO	i^{th} plant outage.
PV	Photovoltaic.
RBA	Ring bus arrangement.
RTDS	Real-Time Digital Simulator.
RTU	Remote terminal unit.
SBA	Single bus arrangement.
SBN	Single-neuron binary classifier neural network.
SCADA	Supervisory control and data acquisition.
SLP	Substation-level processing.
SMRS	Supervisory control and data acquisition system monitoring of relay signals.
SOTA	State-of-the-art.
TCP/IP	Transmission control protocol/internet protocol.
TNTP	Transmission network topology processing.
TNTP-SMRS	Supervisory control and data acquisition system monitoring of relay signal based transmission network topology processing.
α_i	Participation factor for Plant i.
ΔP_{tie}	Tie-line power flow difference from the reference value.
ΔP_{ref}	Total power adjustment required.
$\Delta P_{ref\_plant\ i}$	i^{th} power plant power adjustment required.
ΔT_{Event_S1}	Control trigger delay for the event by SCADA compared to PMU (Scenario 1).
ΔT_{Event_S2}	Control trigger delay for the event by PMU compared to SCADA (Scenario 2).
ΔT_{PMU}	PMU data rate.
ΔT_{SCADA}	SCADA data rate.
λ_R	Balancing authority's bias factor.
a_i	i^{th} branch connectivity status.
ACE	Area control error.
$b_{(i,i)}$	i^{th} node isolation status.
$b_{(i,j)}$	i and j nodes connectivity status.
$f_{substation\ 7}$	Frequency measured at the substation 7.
I_i	i^{th} branch currents.
$I_{(thresh,i)}$	i^{th} branch current threshold.
k	Proportional gain.
$P_{substation\ i}$	Power measured at the substation i for tie-line flow.
P_{ref}	Tie-line power flow reference value.
$P_{Line}(tstop)$	Power flow of *Line* at *tstop*.
$P_{Line}(t)$	Power flow of *Line* at t.
tl	Node voltage measurement tolerance.
T	Time constant.
T_{CM1}	Latency in communicating the measurements from the PMUs/SCADA to the remote server.
T_{CM2}	Latency in communicating the reconfiguration trigger signal from the remote server to the AGC.
T_{CP}	Computational latency.
T_{CP1}	Computational latency for updating the TNTP using either the TNTP-SMRS or H-TNTP-PMU approaches.
T_{CP2}	Computational latency for identifying the outage and initiating the reconfiguration trigger signal based on the updated TNTP.
TEP_{Line}	Transient energy of the *Line* power flow.
$tstart$	Start time of the selected time window.
$tstop$	End time of the selected time window.
V_j	j^{th} node voltages.
$V_{(thresh,j)}$	j^{th} node voltage threshold.

I. INTRODUCTION

Transmission network topology processing (TNTP) identifies the transmission network components' connectivity at the energy control center (ECC). The TNTP is the basis for multiple energy management system (EMS) applications, including operational, security [1], [2], [3], and electricity market [4], [5]. The state-of-the-art (SOTA) TNTP utilizes supervisory control and data acquisition (SCADA) based monitoring of relay signals (SMRS). SMRS is collected by the remote terminal units (RTUs) in substations [6] and telemeter through transmission control protocol/internet protocol (TCP/IP) or inter-control center communications protocol (ICCP) [7]. SMRS-based SOTA TNTP (TNTP-SMRS) can only update the network topology at around 2-5s [8]. Initially, in the TNTP-SMRS process, the breaker statuses are used to build the node-branch model (NBM), which is translated to the dynamic network bus-branch model (BBM) after excluding zero or near-zero impedance branches from the NBM [9]. The EMS operational applications use network BBM as the fundamental topology of the network. More details on TNTP and usage in power system operation can be found in [10].

The modern power system is evolving rapidly. The bulk power system is integrated with grid-connected inverter-based resources such as solar photovoltaic (PV) and wind. The aggregated effect of the active distribution systems, including the rapid integration of distributed energy resources (DER), the introduction of demand response (DR) programs, the rapid growth of commercialized electrical vehicles (EVs), and the integration of microgrids is reflected at the substations, which eventually influence the transmission network operation. The modern power system transmission network is highly dynamic due to these power system upgrades [11]. Furthermore, flexible network reconfiguration is preferred in the modern bulk power system [12]. Thus, reliable and fast TNTP is essential for modern power system operation and control. EMS applications based on TNTP, such as state estimation [13], security-constrained dynamic

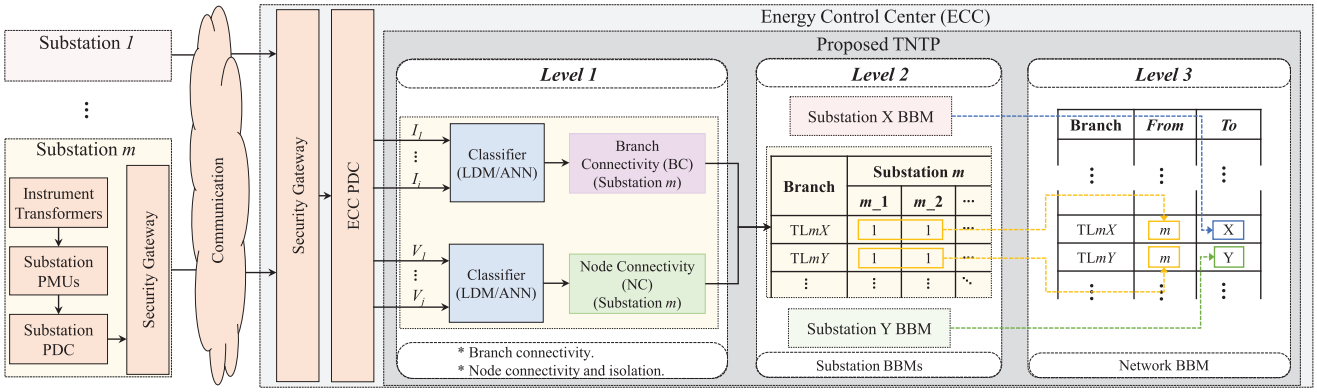

FIGURE 1. The proposed three-level hierarchical TNTP (H-TNTP) approach considering substation *m* as an example.

optimal power flow [14], and automatic generation control (AGC), a faster TNTP approach is favorable.

The main contributions of this paper are:

- A literature review on TNTP is presented, identifying the shortcomings of the current SOTA and alternative approaches proposed by other researchers.
- An efficient and reliable three-level hierarchical TNTP (H-TNTP) approach is proposed using artificial intelligence algorithms, as shown in Fig. 1. This integrates substation configuration identification (CI) of all typical substation arrangements derived from branch current and node voltage measurement.
- Fast frequency regulations by AGC reconfiguration based on the proposed H-TNTP for contingencies is illustrated. Typical results are presented for the proposed AGC reconfiguration compared to the SOTA.

The rest of the paper is organized as follows: Section II presents a literature review on TNTP. Section III briefly overviews different substation arrangements and the modified two-area four-machine power system test model. Section IV elaborates on the methodology of the proposed H-TNTP approach. Typical results for topology processing and the performance improvement achieved with the H-TNTP-PMU based fast AGC reconfiguration are demonstrated in Section V. The conclusion and future directions are provided in Section VI.

II. CURRENT AND PROPOSED WORK

A. SOTA TNTP

A review of the SOTA TNTP and the available literature is presented in [7] and [15], which analyzes the shortcomings of the available literature and the TNTP-SMRS approach. The review emphasizes the following main issues: the inefficiency of the TNTP-SMRS method, the absence of a complete approach for topology processing in the literature, a limited number of studies that have considered substation arrangements in the proposed approaches, and the insufficiency of robustness. H-TNTP effectively ventures all the previously mentioned concerns. It presents a comprehensive topology processing architecture encompassing all typically used substation arrangements. Moreover, H-TNTP utilizes synchrophasor network (H-TNTP-PMU) to establish an efficient and reliable TNTP.

Verification of TNTP-SMRS based on the state estimation outcomes is proposed in [16], [18], and [28], which is a feedback approach that annexes further unfavorable delays to the inefficient TNTP-SMRS. In H-TNTP, inherent verification is conducted along with the TNTP procedure. Topology processing with a fuzzy c-means algorithm using line flows and power injection quantities is presented in [17]. The proposed approach presented in [17] adopts pattern recognition training to identify the topology changes, which can be computationally demanding for a relatively simple problem. H-TNTP employs straightforward, intelligent modules at the primary level of the procedure to understand node and branch connectivity within substations. By utilizing computationally light techniques, H-TNTP significantly reduces computational time, allowing the establishment of future H-TNTP-based comprehensive applications under the data sampling rate. Real-time TNTP based on new circuit breaker monitoring architecture is proposed in [19]. Upgrading the substations with new communication infrastructure is costly and time-consuming, which is not required in the H-TNTP. H-TNTP utilizes existing node voltage and branch current measurements through synchrophasor, telemetered analog measurements from RTUs or synchronized point-on-wave data. A new algorithm to analyze the topology utilizing PMU measurements is proposed in [20], which relies on TNTP-SMRS that introduces the same limitations. Common information model (CIM) based software application developed for TNTP presented in [21] is based on the standard SCADA telemetry as the data source and proposed new cyber model for TNTP. In comparison, the H-TNTP focused on the power system's existing telemetry infrastructure and cyberinfrastructure to derive robust TNTP in a similar format to the SOTA, which allows straightforward integration to the EMS. The use of PMU measurements to derive topology for implementing a linear state estimator (LSE) was studied in [22], where the test

TABLE 1. Topology processing literature review summary.

Index	Reference (Year)	Modification		Data source			Approach						
		Software	Hardware	SCADA	Synchrophasor	Alternative	Comprehensive (Levels in Fig.1)			Complexity	Robust	Verification	Speed
							1	2	3				
1	[16] (2004)	Yes	No	No	No	Yes	Yes	Yes	Yes	High (Classical)	-	Yes	Medium
2	[17] (2005)	Yes	No	Yes	No	No	No	No	Yes	Medium (AI-based)	-	Yes	Low
3	[18] (2006)	Yes	No	No	No	Yes	Yes	Yes	Yes	High (Classical)	-	Yes	-
4	[19] (2006)	Yes	Yes	No	No	Yes	Yes	Yes	Yes	Medium (Classical)	-	-	-
5	[20] (2010)	Yes	No	Yes	Yes	No	Yes	Yes	Yes	Medium (Classical)	-	-	Low
6	[21] (2011)	Yes	No	Yes	No	No	No	No	Yes	Medium (Classical)	-	-	Low
7	[22] (2013)	Yes	Yes	No	Yes	No	Yes	Yes	Yes	Low (Classical)	-	Yes	-
8	[23] (2014)	Yes	No	Yes	No	No	Yes	Yes	Yes	Medium (Classical)	-	-	Low
9	[24] (2014)	Yes	No	No	Yes	No	No	No	Yes	High (Classical)	-	-	-
10	[25] (2017)	Yes	No	Yes	No	No	Yes	Yes	Yes	Medium (Classical)	-	-	Low
11	[26] (2020)	Yes	No	No	No	Yes	Yes	Yes	Yes	High (Classical)	-	-	Low
12	[27] (2021)	Yes	No	Yes	No	No	No	No	Yes	High (AI-based)	-	Yes	Low
13	[28] (2022)	Yes	No	No	No	Yes	Yes	Yes	Yes	High (Classical)	-	Yes	-
14	TNTP-SMRS	No	No	Yes	No	No	Yes	Yes	Yes	Low (Classical)	-	-	Low
15	H-TNTP-PMU	Yes	No	No	Yes	No	Yes	Yes	Yes	Low (AI-based)	Yes	Yes	High

"Yes" indicates that literature is satisfying the considering property, "No" indicates it is not satisfying, and "-" indicates indeterminate with the information available.

system uses the breaker status as a digital input to the PMU. Digital inputs in the PMUs will require additional communication network upgrades from RTUs to PMUs in the substation. An efficient topology processing for state estimation proposed in [23] is based on SMRS. The use of SMRS still limits the speed of TNTP and neglects the possibility of equipment malfunctions in the substations. H-TNTP is a physics-based approach that is unsusceptible to equipment malfunctions. A topology estimation approach utilizing log-spline copulas established with Monte Carlo simulations with PMU measurements is presented in [24]. This study did not consider substation arrangements, simplifying the topology estimation problem to branch outage detection. H-TNTP considers all typically used substation arrangements, allowing topology processing under different substations' dynamic configurations. The paper [25] studies network topology processing at the substation level (SLP) using SMRS. Subsequently, the SLP is integrated into network-level processing (NLP). In comparison, the H-TNTP procedure adopts an extended, comprehensive three-level structure and intentionally avoids using SMRS to overcome its associated shortcomings. An optimal network topology processing considering power flow constraints is presented in [26]. In this approach, the computation process is rigorous, which will delay the topology processing. Furthermore, the paper presents complete results for a breaker and half arranged substation as an example. It is crucial to present the results for all typically used substation arrangements. Knowledge graph and graph neural network-based power system network topology identification presented in [27] has overlooked the substation arrangements, leading to a simplified topology processing problem focused solely on branch status identification. Nevertheless, this assumption of assuming a substation as a single node in modern power system operation is not acceptable. Substation configuration plays a crucial role in utility operations for controlling power flow, network reconfiguration, and enabling network splitting and islanding.

A summarized qualitative literature comparison with SOTA and the H-TNTP-PMU is organized chronologically in Table 1. All literature proposed approaches are investigated for the required ''Modification'' in the power system under the ''Software'' and ''Hardware'' categories. The ''Data source'' implies the method used to provide the required input data/measurement for the approach. The source of data can be from fundamental telemetry sources such as ''SCADA,'' ''Synchrophasor,'' or ''Alternative'' data sources such as virtual sources (state estimation output) or dedicated network communications. The approaches are investigated further under comprehensiveness and complexity. ''Comprehensive'' denotes the approach proposed as a complete TNTP tool or a sublevel of the TNTP according to the three levels of the H-TNTP as shown in Fig. 1. ''Complexity'' describes the algorithm complexity level of the proposed approach and

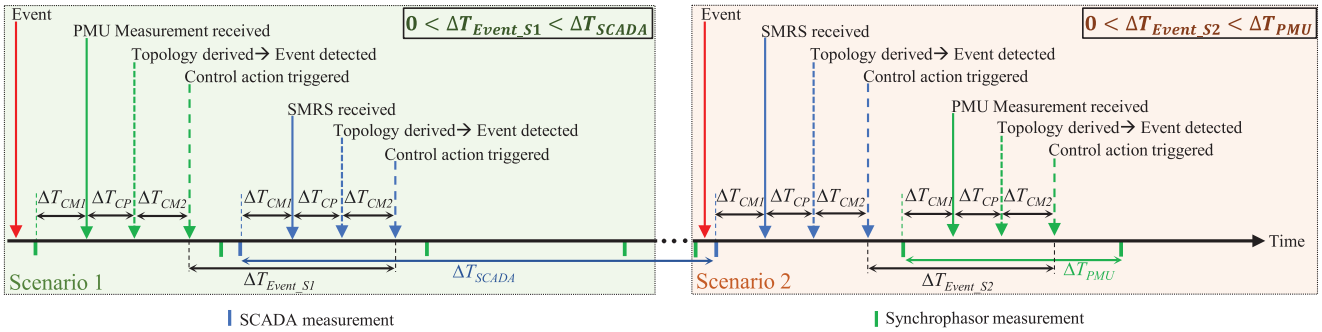

FIGURE 2. Efficiency comparison of control actions based on H-TNTP-PMU and TNTP-SMRST approaches considering the uncertainty of the event occurrence instant on the timeline.

distinguishes between "AI-based" or "Classical" (non-AI) approach. Furthermore, "Robust" indicates whether the approach is performed as intended under breaker/manual switch/relay malfunctions, cyber/physical attacks, or false manual switch operations caused by human errors. All proposed approaches were examined regarding incorporating a validation procedure under the title "Verification." The "speed" in Table 1 refers to the overall estimated time taken by the different approaches based on the type of communication method used and the computational overhead of the algorithm deployed.

B. PROPOSED TNTP

The proposed H-TNTP addresses the limitations discussed in the existing literature by introducing a hierarchical structure for enhanced scalability. This innovative framework can integrate with telemeter technologies, including synchrophasor, analog measurements through SCADA or synchronized point-on-wave data that provides branch current and node voltage measurements. The reliability of the H-TNTP is ensured via in-built verification, which avoids erroneous results. Since the proposed approach is based on the physics of electrical circuits, manual switch (isolators) operations in the substations are included in TNTP by default. Moreover, unlike TNTP-SMRS, a malfunctioning breaker/manual switch/relay will not lead to incorrect topology in H-TNTP. Thus, the reliability of TNTP is improved. Artificial intelligence (AI) algorithms are utilized for decision-making. H-TNTP adapts all typically used substation arrangements, ensuring its practical applicability.

H-TNTP updates network BBM in every measurement frame. PMUs measure voltage and current phasors at a higher frequency (typically at 30Hz) than SCADA (typically every 2s-5s), which supports the establishment of a fast TNTP. Due to the uncertainty of when the network topology may change, two possible scenarios in the topology identification-based flow can be defined, as shown in Fig. 2. The occurrence of Scenario 1 is more common since the PMU measurement rate is at least 60 times higher than the SCADA rate. The maximum delay of the PMU-based command trigger for Scenario 2 compared to the SCADA-based command trigger (ΔT_{Event_S2}) is the PMU measurement rate (33.33ms at 30Hz). The maximum delay of the SCADA-based command trigger for Scenario 1 compared to the PMU-based command trigger (ΔT_{Event_S1}) is high as the SCADA measurement rate (around 2s), which further justifies the use of synchrophasor measurements for fast H-TNTP.

III. POWER SYSTEM WITH SUBSTATION ARRANGEMENTS

Transmission network topology processing is solely based on the substation arrangement. The modified two-area four-machine power system model with all typically used substation arrangements is shown in Fig. 3. Substation configurations are summarized in Table 2. The model consists of four conventional power generation plants and two PV plants. Plant 1, with three 300MVA generators, is connected to Substation 5. Plant 2, with 500MVA and 400MVA generators, is connected to Substation 6. Plant 3, with three 300MVA generators, is connected to Substation 11, and Plant 4, with two 450MVA generators, is connected to Substation 10. Each solar PV plant is rated at 600MW. PMUs are installed in each substation to measure the node voltages and branch currents. Thus, current phasor measurements of each branch connecting to any substation and node voltages are available at the substation control room and the ECC. Substations in the transmission network are configured for different arrangements. All conventional generators are configured with turbine governors, automatic voltage regulators, and power system stabilizers. Both Area 1 and Area 2 in the model are configured with reconfigurable AGCs. The simulation is carried out using the RSCAD software on the Real-Time Digital Simulator (RTDS) [30]. RSCAD software PMUs are utilized for this study.

Substations are used to control the connectivity of the power system components. Substation CI depends on the substation's designed arrangement. Single bus arrangement (SBA) is the fundamental arrangement type. The reliability of SBA is low due to a lack of redundancy under breaker, isolator failure, or bus fault. All the branches are directly connected to a single bus through a circuit breaker and an isolator. Main and transfer bus arrangement (MTBA) is designed to connect all branches between the main and transfer buses. At any point

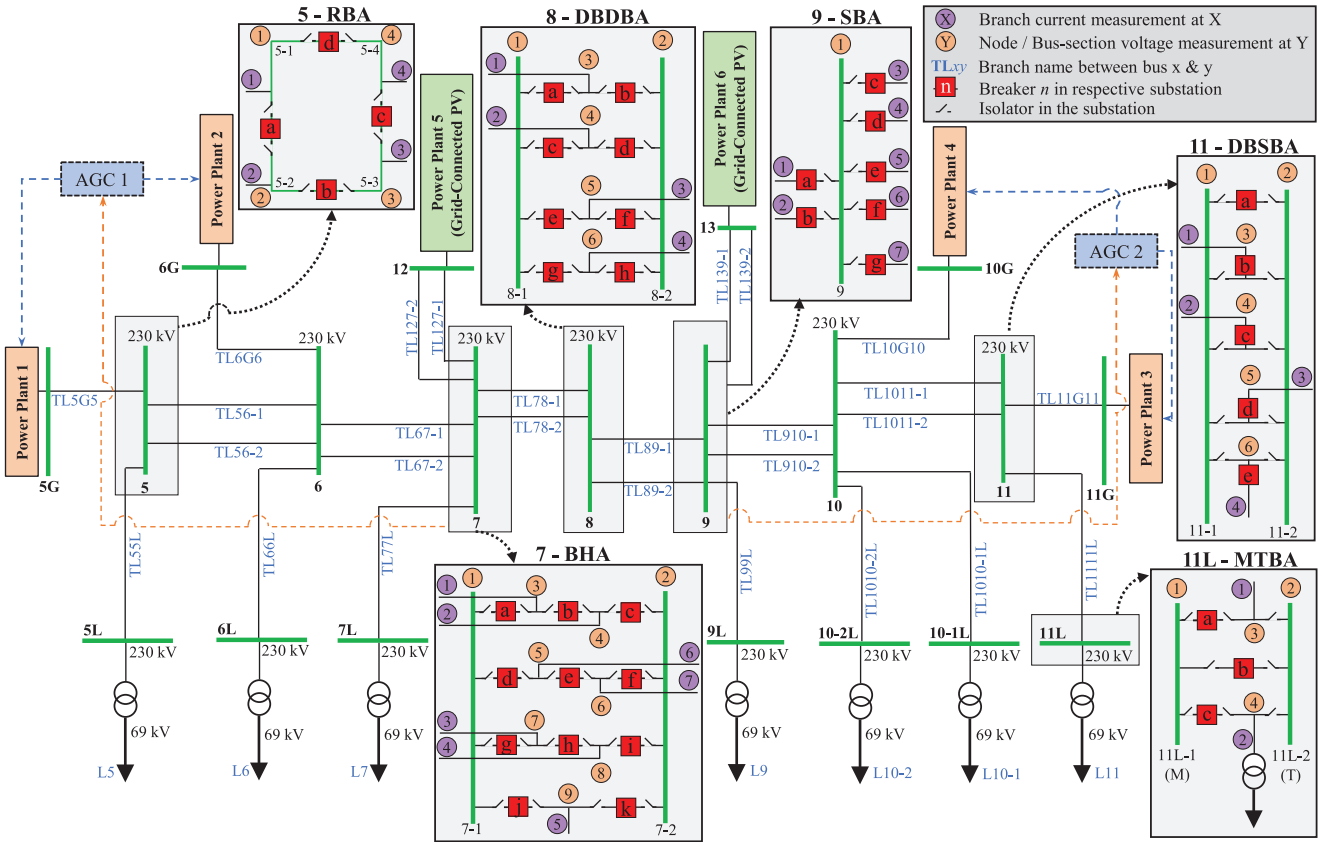

FIGURE 3. Modified two-area four-machine power system model with substation arrangements [29] and reconfigurable automatic generation controls (AGCs).

TABLE 2. Modified two-area four-machine power system model substation configuration summary.

Substation ID	Substation type	Branches	Breakers	Isolators	PMU measurements	
					Voltage	Current
5G	SBA	2	2	2	1	2
5	RBA	4	4	8	4	4
5L	SBA	2	2	2	1	2
6G	SBA	2	2	2	1	2
6	SBA	6	6	6	1	6
6L	SBA	2	2	2	1	2
7	BHA	7	11	22	9	7
12	SBA	3	3	3	1	3
7L	SBA	2	2	2	1	2
8	DBDBA	4	8	16	6	4
9	SBA	7	7	7	1	7
13	SBA	3	3	3	1	3
9L	SBA	2	2	2	1	2
10G	SBA	2	2	2	1	2
10	SBA	7	7	7	1	7
10-1L	SBA	2	2	2	1	2
10-2L	SBA	2	2	2	1	2
11G	SBA	2	2	2	1	2
11	DBSBA	4	5	10	6	4
11L	MTBA	2	3	8	4	2

of active operation, branches connecting to the main bus can be transferred to the transfer bus, and the substation can be operated without interruption. Ring bus arrangement (RBA) is built by bus sections (branch nodes), which are connected through circuit breakers and two isolators segment. Any segment malfunction does not affect the substation operation, which makes RBA a moderately reliable arrangement. A combination of multiple circuit breaker operations is

utilized to reconfigure the component connectivity. Double bus single breaker arrangement (DBSBA) is a moderately reliable substation arrangement, where isolator failures will not result in system interruptions, although breaker failures will interrupt the power system operation. All branches are connected to both bus nodes through a single breaker and two isolators segment. Double bus double breaker arrangement (DBDBA) is a highly reliable arrangement. Each branch is connected through two segments of two isolators and a single breaker to the two bus nodes. Thus, any segment failure will not interrupt the power system operation. Breaker and half arrangement (BHA) is a highly reliable arrangement, where every two branches in the substation are connected through three segments of two isolators and a single breaker to the two bus nodes. Thus, failure of any segment will not affect the power system operation.

IV. AI BASED TRANSMISSION NETWORK TOPOLOGY PROCESSING APPROACH

The H-TNTP approach shown in Fig. 1 consists of three levels as described below.

1) Level 1:
   a) Determination of branch connectivity and formation of branch connectivity matrices (BCMs) for the substations.
   b) Determination of node connectivity and isolation statuses and formation of node connectivity matrices (NCMs) for the substations.

2) Level 2: Integration of BCM and NCM and formation of BBM for the substations.

3) Level 3: Integration of all substation BBMs to establish the network BBM.

A. LEVEL 1: BRANCH CONNECTIVITY IDENTIFICATION

The objective of Level 1 of the H-TNTP is to derive substations BCM and NCM. The BCM is the connectivity status of all branches to the substation that is identified by the classifier using branch current measurements. Two AI algorithms are used as classifiers for Level 1. Logical procedures for decision-making can be established with expert knowledge, which is the foundation of the logical decision-making (LDM) algorithm, and an artificial neural network (NN) classifier can be established based on a generic training data set.

According to the physics of electric circuits, a branch disconnection from the circuit will result in zero current. Although, a small current can be available due to residual charges or magnetic flux. Considering both physics knowledge and practical perspective, the branch current measurements are pre-processed by comparing to the threshold ($I_{thresh,i}$) defined by the expert into the binary format. If the branch's current measurement is less than or equal to the defined threshold value, binary variable A is set to 0; otherwise, A is set to 1. Expert-defined thresholds to infer

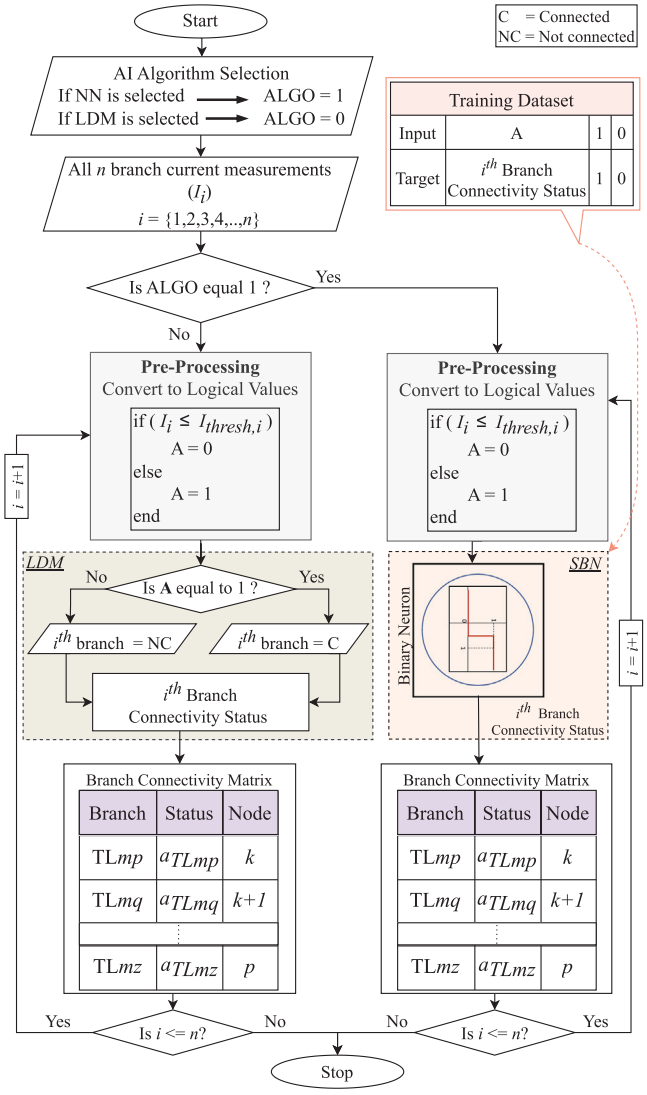

FIGURE 4. Branch connectivity matrix (BCM) derivation flow diagram for all substation arrangements.

decisions are used in the process of BCM derivation using LDM, as shown in Fig. 4, which is integrated to form the BCM based on (1). Neural networks can be used for learning accurate decision rule sets. Since the derivation of BCM is a simple classification problem, a single-neuron binary classifier neural network (SBN) is utilized as algorithm. The binary neuron will accept a similar input as the LDM approach and classify the branch connectivity. In the NN classifier training process, weights are adjusted to maximize the accuracy of matching the actual target to the estimated target. Further explanation of feed-forward NN for classification can be found in [31]. The physics-based binary variable formation mentioned above is used to derive the SBN training dataset. There can be 2^n possible branch connectivity status combinations despite the stability concerns, where n is the number of branches. Any combination of branch outages, including double circuit lines, can be identified

in the proposed BCM procedure. The BCM procedure is independent of the substation arrangement.

$$a_i = \begin{cases} 1, & \text{if branch } i \text{ is connected} \\ 0, & \text{if branch } i \text{ is disconnected} \end{cases} \quad (1)$$

Identification

B. LEVEL 1: NODE CONNECTIVITY IDENTIFICATION

Substation NCM depends on the substation arrangement type. Substation NCM derivation for commonly used substation arrangement types [29] is explained below.

1) SINGLE BUS ARRANGEMENT

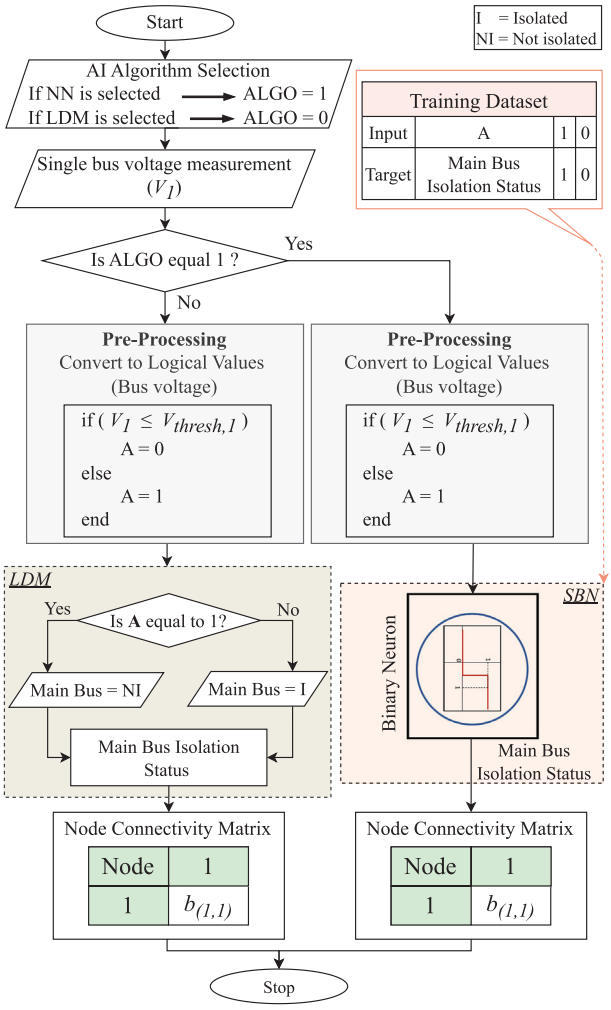

FIGURE 5. Node connectivity matrix (NCM) derivation flow diagram for substation arrangement SBA.

SBA substation only has one main bus. The sole purpose of the NCM of the SBA substation is to identify the main bus isolation status from the network. In practice, an isolated bus or branch node is grounded for safety and protection, which results in zero voltage. In this case, the user can consider $V_{thresh,1} = 0$. In the pre-processing, suppose the main bus node voltage is less than or equal to the expert-defined threshold ($V_{thresh,1}$), set $A = 0$; otherwise, set $A = 1$. NCM is updated based on the main bus node isolation status from (2). The detailed procedure is shown in Fig. 5.

$$b_{(i,i)} = \begin{cases} 1, & \text{if } i^{th} \text{ node is not isolated} \\ 0, & \text{if } i^{th} \text{ node is isolated} \end{cases} \quad (2)$$

2) MAIN AND TRANSFER BUS ARRANGEMENT

MTBA substation can be used in non-critical nodes of the transmission network to connect through and control two or more branches. The MTBA substation functional arrangement (FA) based on substation CI has been described in [32], which is developed further in this study to derive NCM. The voltage measurements are converted to binary format based on the expert-defined threshold ($V_{thresh,i}$). Main and transfer bus interconnectivity is derived from the procedure shown in Fig. 6. B_1 and B_2 are the NN input and hidden layer biases. n is the number of nodes in the MTBA substation. tl is the tolerance of the node voltage measurement, which allows the countering of the instrument error margins. If the selected node voltage is less than or equal to the expert-defined threshold ($V_{thresh,i}$), set $A = 0$; otherwise, set $A = 1$. If the voltages of node i is in between $(V_j - tl)$, and $(V_j + tl)$, set $B = 1$; otherwise, set $B = 0$. NCM is updated based on the node i and j connectivity from (3) and node i isolation status from (2). i and j nodes can be either bus or branch nodes, as shown in Substation 11L in Fig. 3.

$$b_{(i,j)} = \begin{cases} 1, & \text{if } i \text{ and } j \text{ nodes are connected} \\ 0, & \text{if } i \text{ and } j \text{ nodes are not connected} \end{cases} \quad (3)$$

3) RING BUS ARRANGEMENT

The NCM of the RBA is based on the voltage measurements of the bus sections (branch nodes). NCM of the RBA can be formed based on the knowledge of each bus section's connectivity with the other bus sections. NCM can be formed using the flow diagram shown in Fig. 6. n is the number of bus sections in the RBA substation. If the considered branch node voltage is less than or equal to the expert-defined threshold ($V_{thresh,i}$), set $A = 0$; otherwise, set $A = 1$. If the voltages of bus section i is in between $(V_j - tl)$, and $(V_j + tl)$, set $B = 1$; otherwise, set $B = 0$. With the LDM or NN algorithm output, NCM is updated based on the node i and j connectivity from (3) and node i isolation status from (2). i and j are branch nodes, as shown in Substation 5 in Fig. 3.

4) DOUBLE BUS SINGLE BREAKER ARRANGEMENT

NCM of the DBSBA can be formed based on the knowledge of each bus and branch node connectivity and isolation status. This can be derived using the flow diagram shown in Fig. 6. n is the number of nodes in the DBSBA substation. NCM is updated for each measurement frame based on the node i and j connectivity from (3) and node i isolation status from (2).

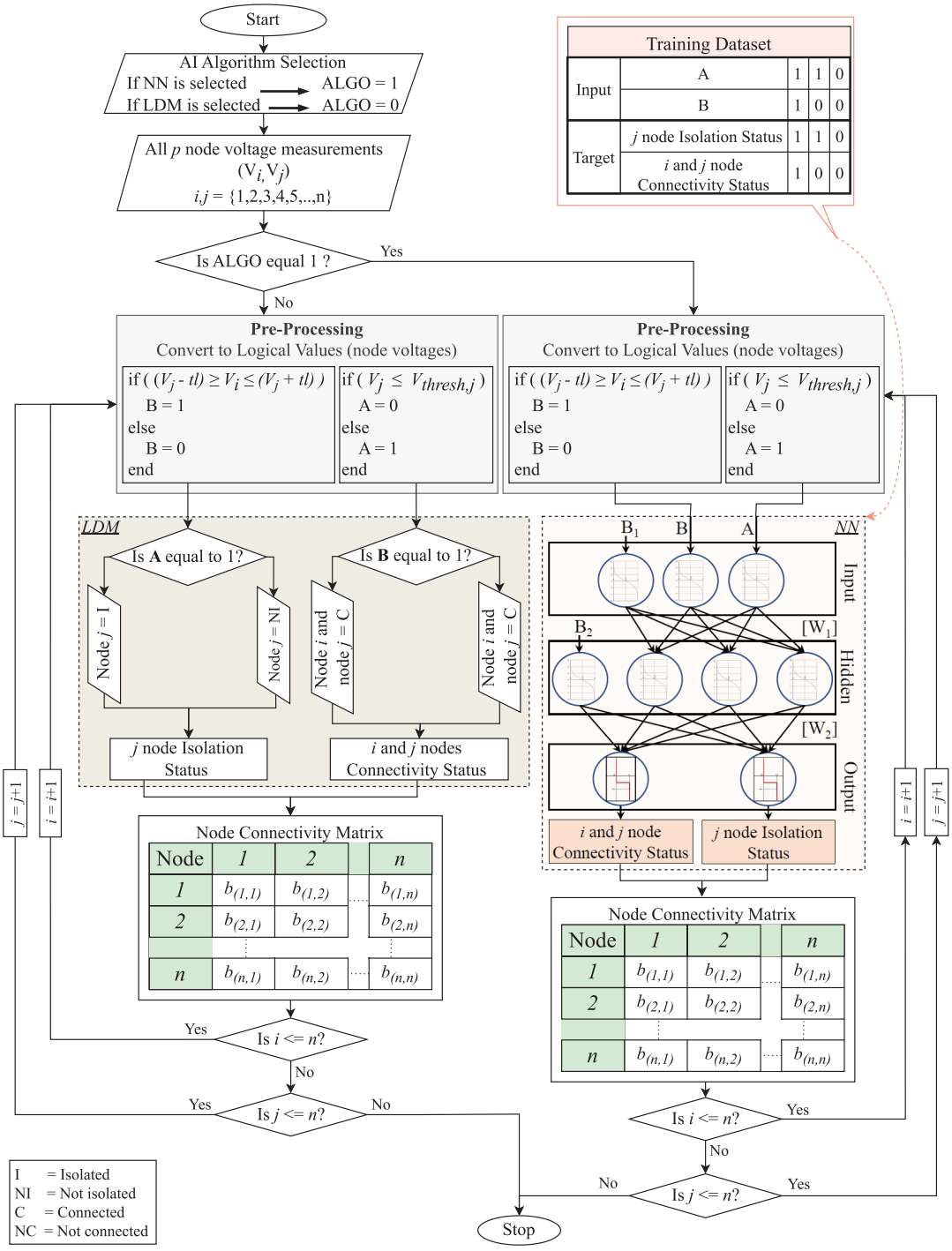

FIGURE 6. Node connectivity matrix (NCM) derivation flow diagram for substation arrangements MTBA, RBA, DBDBA, DBSBA, and BHA.

5) DOUBLE BUS DOUBLE BREAKER ARRANGEMENT

The procedure shown in Fig. 6 can be used to form NCM for DBDBA. Equivalent to DBSBA, the NCM of the DBDBA explains the connectivity and isolation status of all nodes in the substation. Understanding the connectivity between A and B bus nodes in Substation 8 is critical since Substation 8 is responsible for the interconnectivity of Areas 1 and 2. Substation 8 can be utilized for area separation. DBDBA is a flexible substation arrangement that allows ECC to manipulate the branch connectivity in several different configurations. This characteristic is helpful in emergency operations and to accommodate future grid requirements such as flexibility in transmission networks [33].

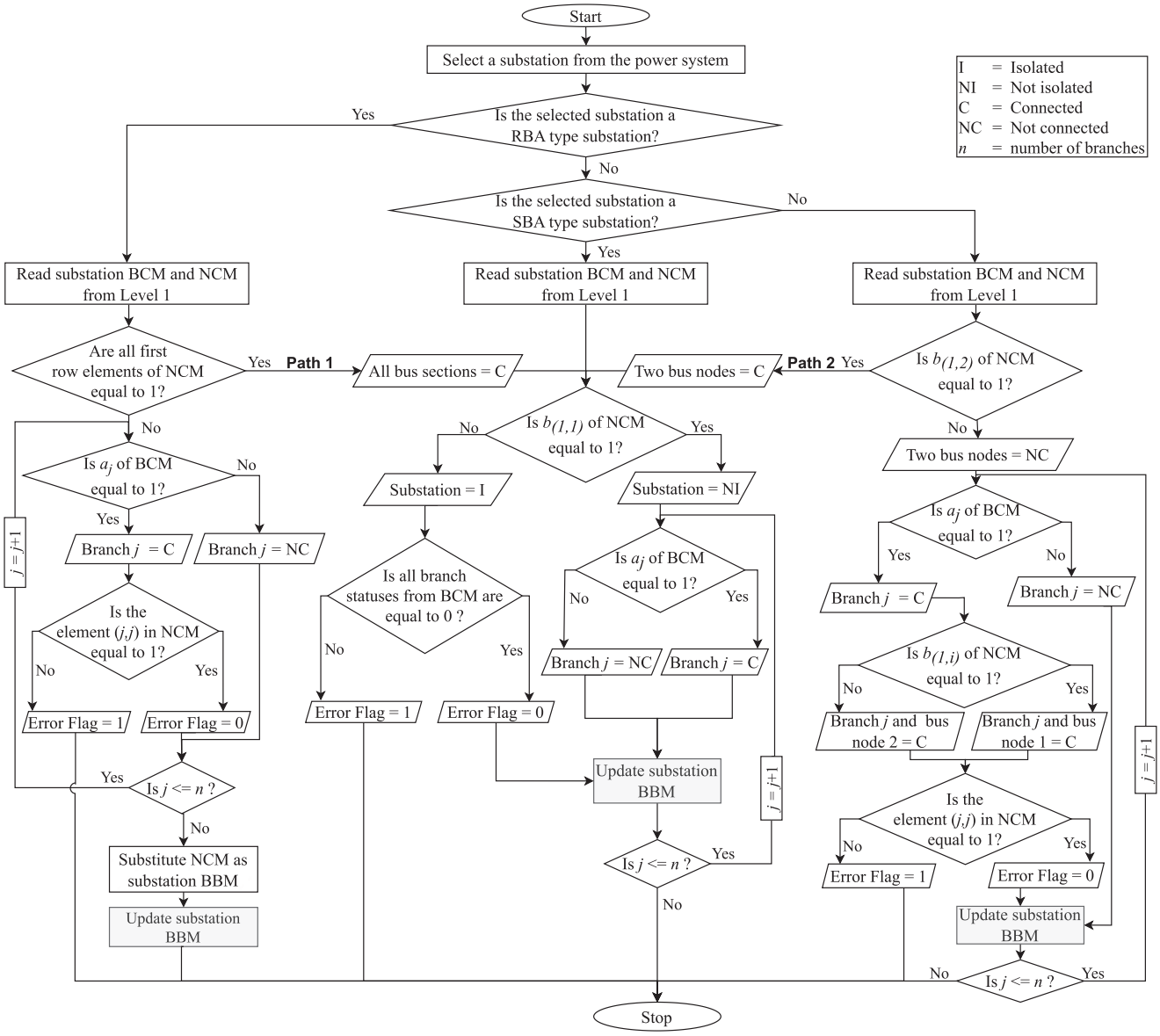

FIGURE 7. Integration of branch connectivity matrix (BCM) and node connectivity matrix (NCM) from Level 1 of the H-TNTP approach to form substation bus branch model (BBM) of Level 2. In the case of all bus nodes in multi-bus node substation arrangements being interconnected, the Level 2 procedure follows Path 1 and Path 2 and is processed as an SBA arrangement.

6) BREAKER AND HALF ARRANGEMENT

Similar to DBDBA, the NCM of the BHA substation can be formed using the procedure shown in Fig. 6, which explains the connectivity of the bus, branch nodes in the substation, and isolation status of all nodes. LDM or NN algorithm can be utilized to derive the elements for the NCM based on (3) and (2). BHA is a commonly used substation arrangement in transmission substations due to its flexibility and reliability.

C. LEVEL 2: SUBSTATION BBM DERIVATION

BCM and the NCM from Level 1 of each substation are integrated by following the procedure shown in Fig. 7 to form the substation BBM in Level 2 of the H-TNTP. Substation CI can be interpreted using the substation BBM. It is important to note that the inherent verification is conducted while forming substation BBMs utilizing the redundancy in NCM and BCM, as shown in Fig. 7. BCM has a column with information about the branch node in the substation where each branch is connected. The inherent verification is based on the ground truth that a branch node should not be isolated if the respective branch is connected to the substation. The isolation of a branch node can be identified from the NCM diagonal element corresponding to the node ID row and column. Thus, a cross-verification can be established.

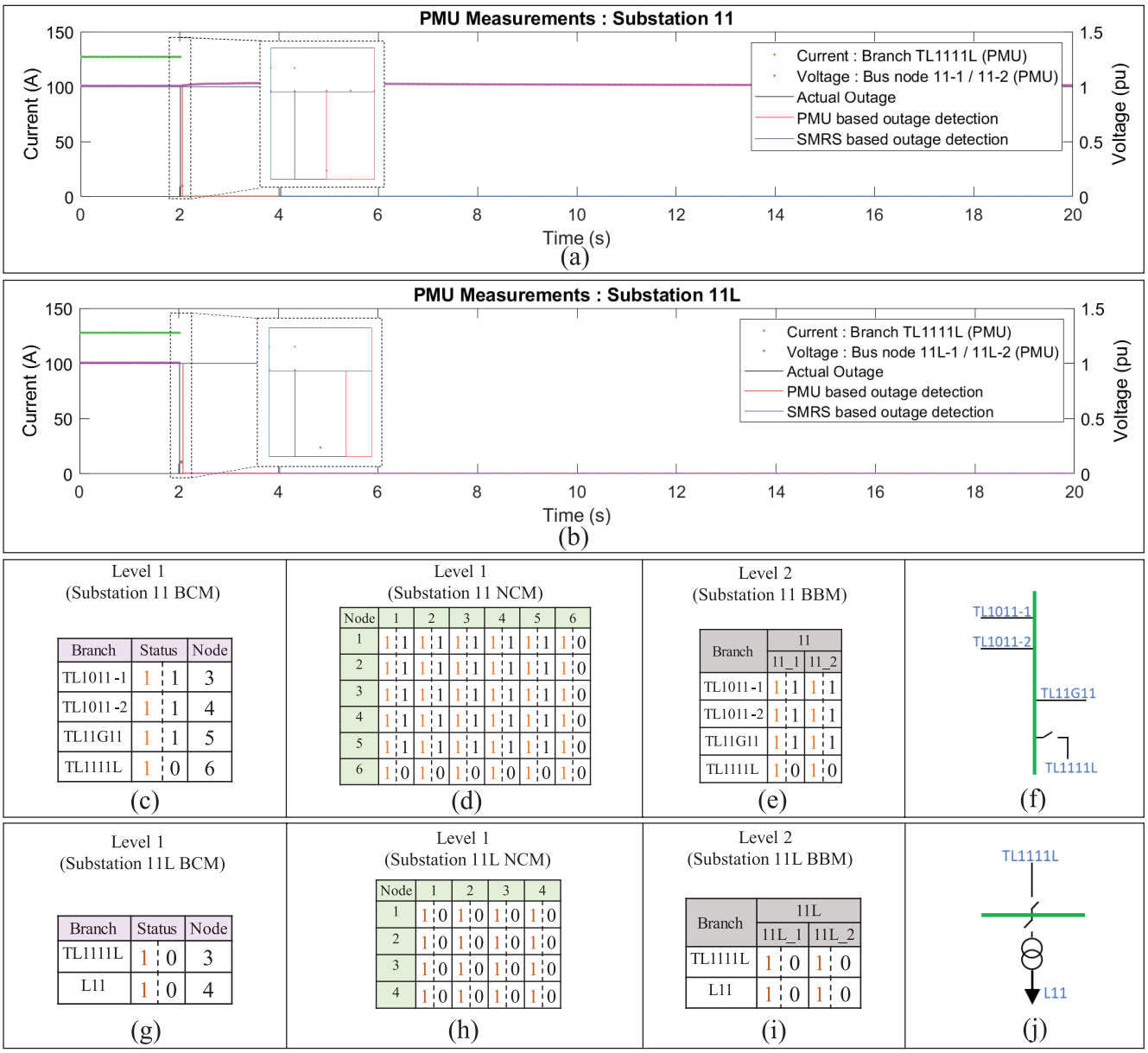

FIGURE 8. Results for the single branch outage of TL1111L, as shown in Fig. 3. (a) TL1111L branch current and 11-1 / 11-2 bus node voltage waveforms from the Substation 11 PMU measurements, (b) TL1111L branch current and 11L-1 / 11L-2 bus node voltage waveforms from the Substation 11L PMU measurements, (c) Derived BCM at Level 1 for Substation 11, (d) Derived NCM at Level 1 for Substation 11, (e) Formed BBM for Substation 11 at Level 2, (f) Resultant FA [32] for Substation 11, (g) Derived BCM at Level 1 for Substation 11L, (h) Derived NCM at Level 1 for Substation 11L, (i) Formed BBM for Substation 11L at level 2, (j) Resultant FA [32] for Substation 11L.

D. LEVEL 3: NETWORK BBM ESTABLISHMENT

Level 3 of the H-TNTP aims to integrate all substation BBMs to establish the network BBM, which is achieved by updating each branch row in the network BBM. Substation BBMs of the respective branch's two ends are investigated to understand the branch connectivity with the substation nodes. If the substation bus nodes are interconnected, the substation ID is updated as the network BBM's respective *From* or *To* column. The respective bus node ID is updated if the substation bus nodes are separated. In the RBA substation, where more than two bus nodes are available, all interconnected bus-node IDs (bus sections) are updated under the respective *From* or *To* column. If a branch is not connected, the *From* and *To* columns under the respective branch are updated as −. Update for the TL78-1 row of the network BBM during two bus nodes of Substation 7 are separated while two bus nodes of Substation 8 are interconnected conducted as follows: branch TL78-1 is configured to transmit power from Substation 7 to Substation 8. Since two bus nodes in Substation 7 are separated, and TL78-1 is connected to 7_1 bus node, the *From* column under the TL78-1 is updated as 7_1. Since two buses in

Substation 8 are interconnected, the *To* column under the TL78-1 is updated as 8.

Update for the TL56-1 and TL55L rows of the network BBM during the TL55L branch is disconnected while all other system components are operating nominally is conducted as follows: branch TL56-1 is configured to transmit power from Substation 5 to Substation 6, and the TL55L is configured to transmit power from Substation 5 to Substation 5L. Since TL55L is disconnected, row TL55L of the network BBM is updated with 0s for both *From* and *To* columns. The TL56-1 row is updated with all the bus sections interconnected in the RBA as 5_1/5_3/5_4. The substation BBM integration to form network BBM in Level 3 of the H-TNTP procedure is programmed to follow the above-explained routine. Thus, changes in substation BBM are automatically reflected in the network BBM.

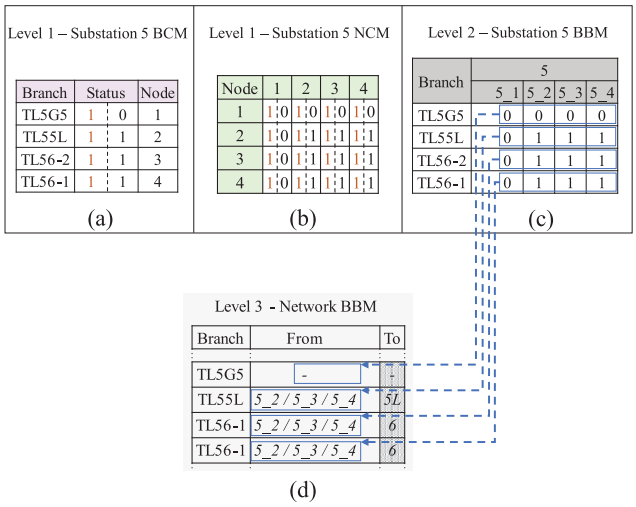

FIGURE 9. Level 1, 2 and 3 results of the H-TNTP procedure for Plant 1 outage. (a) Derived BCM at Level 1 for Substation 5, (b) Derived NCM at Level 1 for Substation 5, (c) Formed BBM for Substation 5 at Level 2, (d) Updated network BBM at Level 3 for the branch outage.

V. RESULTS AND DISCUSSION

The H-TNTP proposed in Section IV is illustrated on the power system shown in Fig. 3. The power system is simulated on the RTDS. The computational modules for the overall procedure are developed in MATLAB.

A. AI-BASED TRANSMISSION NETWORK TOPOLOGY PROCESSING

The following results are presented for single branch outage, plant outage and area separation of the bulk power system. Furthermore, the case studies are established to include all six substation arrangements.

1) CASE STUDY 1—SINGLE BRANCH OUTAGE

The TL1111L transmission line between Substations 11 and 11L (Fig. 3) is disconnected from the network, with the system remaining stable. At each measurement frame, the BCM and the NCM are formed for all substations. The pre-outage matrix values are shown in orange, and the post-outage values are shown in black in Figs. 8 and 9. It is shown in Fig. 8 (a) and (b) how the PMU and SMRS measurements of Substations 11 and 11L support the formation of BCM and NCM. The formed BCM and the NCM for Substation 11 from the H-TNTP Level 1 procedure are shown in Figs. 8c and d, respectively. The post-outage BCM shows that the TL1111L is disconnected from Substation 11. The post-outage NCM shows that the substation is connected to the network. BBM for Substation 11 is formed from the H-TNTP Level 2 procedure using derived BCM, and NCM is shown in Fig. 8 (e).

Post-outage Substation 11 FA is shown in Fig. 8 (f). The formed BCM and the NCM for Substation 11L are shown in Figs. 8 (g) and (h), respectively. The post-outage BCM shows that the TL1111L is disconnected from Substation 11L. The post-outage NCM shows that Substation 11L is disconnected from the network. BBM for Substation 11L is formed from the H-TNTP Level 2 procedure using derived BCM, and NCM is shown in Fig. 8 (i). Substation 11L post-outage FA is shown in Fig. 8 (j). Furthermore, from Figs. 8 (a) and (b), it can be observed that the PMU measurements detect the outage much earlier than the SMRS.

2) CASE STUDY 2—PLANT OUTAGE

The TL5G5 line connecting Plant 1 to Substation 5 in Fig. 3 is disconnected, resulting in the outage of Plant 1. The system remains stable with this plant outage. The pre-outage and post-outage BCM and NCM for Substation 5 are formed, as shown in Figs. 9 (a) and (b), respectively.

The post-outage BCM shows that the TL5G5 line is disconnected from Substation 5. The post-outage NCM shows that Substation 5, node 1 (branch node for TL5G5), is disconnected from the substation. Post-outage Substation 5 BBM shown in Fig. 9 (c) is formed following the procedure explained in Section IV-C. The post-outage network BBM is shown in Fig. 9 (d).

3) CASE STUDY 3—AREA SEPARATION

Tie-line transmission lines, TL78-1, TL78-2, TL89-1, and TL89-2, between Substations 7, 8, and 9 in Fig. 3 are disconnected from the network with the system remaining stable. This separates the two areas of the power system. Consequently, isolating Substation 8 from the rest of the system. Post-outage substation BBMs for Substations 7, 8, and 9 were formed, as shown in Fig. 10 (a), (b), and (c), respectively. Furthermore, the post-outage substation BBMs are integrated to update the network BBM for the area separation, as shown in Fig. 10 (d).

A comparison of TNTP-SMRS and H-TNTP-PMU (Levels 1, 2, and 3) with both LDM and NN algorithms is shown in Table 3. A comprehensive time analysis for H-TNTP-PMU

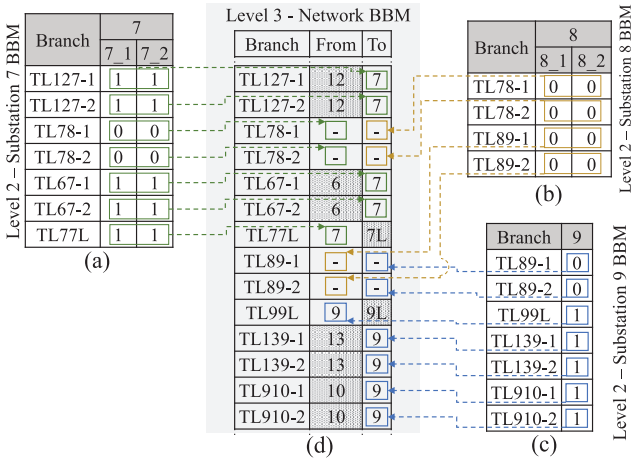

FIGURE 10. Level 2 and 3 results of the H-TNTP procedure for the area separation. (a) Formed BBM for Substation 7 at Level 2, (b) Formed BBM for Substation 8 at Level 2, (c) Formed BBM for Substation 9 at Level 2, (d) Updated network BBM at Level 3 for the area separation.

TABLE 3. Comparison of TNTP with TNTP-SMRS and H-TNTP-PMU approaches.

Factor	TNTP-SMRS	H-TNTP-PMU	
		LDM	NN
Data sampling rate	2s	33.33ms	
Computational Time (μs)[a]	1.0478 $\pm$0.0249	11.3749 $\pm$0.6562	27.5432 $\pm$0.2690
Inherent verification	No	Yes	
Substation isolator operations	No	Yes	
Time synchronization	No	Yes	
Parallel processing	No	Yes (Level 1 and Level 2)	

[a] The computational time for TNTP-SMRS and H-TNTP-PMU (Levels 1, 2, and 3) was calculated on a system with Intel Xeon(R) Gold 3.3GHz with 63.7GB RAM.

TABLE 4. Parameters of AGCs in Area 1 and Area 2 (Fig. 3) [34].

Parameter	AGC1	AGC2
λ_R	20	20
T	0.5	0.5
k	-0.007	-0.007
α_1	[0,0.5,1]	-
α_2	[0,0.5,1]	-
α_3	-	[0,0.5,1]
α_4	-	[0,0.5,1]

based fast AGC reconfiguration is presented in Section V-B, demonstrating the overall efficiency improvement.

B. FAST AGC RECONFIGURATION DURING CONTINGENCY

H-TNTP can be utilized in power system operation applications, including AGC reconfiguration. Any transmission network topology change can be detected at Level 3 network BBM. The laboratory setup for studying the speed of AGC reconfiguration is shown in Fig. 11. The test system has reconfigurable AGCs for Areas 1 and 2 (Fig. 12). AGC parameters are shown in Table 4. PMU measurements are collected at 30Hz, and SMRS are collected every 2s. The reconfiguration trigger signal to the respective AGCs is sent from the ECC based on topology update by either the H-TNTP-PMU or TNTP-SMRS and an outage detection module.

The plant outages and area separation case studies, which require AGC reconfiguration, are considered to compare the performance of the AGC with the TNTP-SMRS and the H-TNTP-PMU.

1) PLANT OUTAGES

Two conventional power plant outages in each area are separately investigated. In each plant outage, AGC is reconfigured to dispatch the imbalanced power from the other plants based on the reconfiguration signal from either H-TNTP-PMU based outage detection or TNTP-SMRS based outage detection. The AGC reconfiguration is conducted only on the power plants of the affected area, as shown in Fig. 12. Under the Plant 1 outage (P1O), AGC 1 is reconfigured to increase Plant 2 dispatch using the coordinated switches by adjusting the participation factors. Coordinated switches need to change to position 2 (*Plant 1 outage*) from 1 (*Normal operation*). Area 2 AGC is not affected. Similarly, for the Plant 3 outage (P3O), AGC 2 is reconfigured accordingly. The resultant power and frequency variations for H-TNTP-PMU and TNTP-SMRS approaches under Plant 1 outage are shown in Fig. 13 and under Plant 3 outage are shown in Fig. 14.

2) AREA SEPARATION

Tie-line bias control is integrated into the Area 1 AGC. Therefore, Area 1 AGC is reconfigured to reflect the tie-line outage, as shown in Fig. 12. Area 1 and 2 AGCs are reconfigured for area frequency regulation in the post-outage. Area 2 AGC is not affected due to the tie-line outage. The resultant power and frequency variation for H-TNTP-PMU and TNTP-SMRS approaches under area separation are shown in Fig. 15.

Fifty trials were conducted for each of the case studies mentioned above to evaluate the speed of AGC reconfiguration. From these trials, it is observed that the H-TNTP-PMU is faster, as shown in Fig. 16 based on the *Total time* (given in (4)) for H-TNTP-PMU and TNTP-SMRS. Furthermore, LDM is more efficient than the NN algorithm, although both approaches are acceptable for fast operational applications based on minimal computational time.

$$Total\ time = T_{CM1} + T_{CP1} + T_{CP2} + T_{CM2} \quad (4)$$

Total time accounts for the time taken to trigger the AGC reconfiguration from the occurrence of the event, T_{CM1} is the latency in communicating the measurements from the PMUs/SCADA to the remote server in Fig. 11, T_{CM2} is the latency in communicating the reconfiguration trigger signal from the remote server to the AGC, T_{CP1} is the computational latency for updating the TNTP using either the TNTP-SMRS or H-TNTP-PMU approaches and, T_{CP2} is the computational

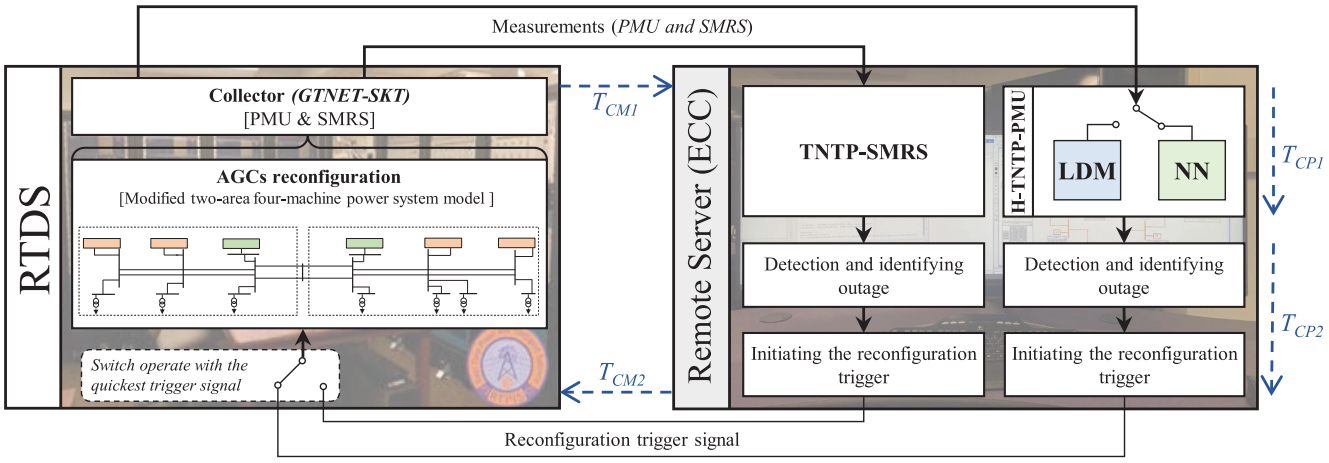

FIGURE 11. Experimental setup for carrying out AGC reconfiguration studies.

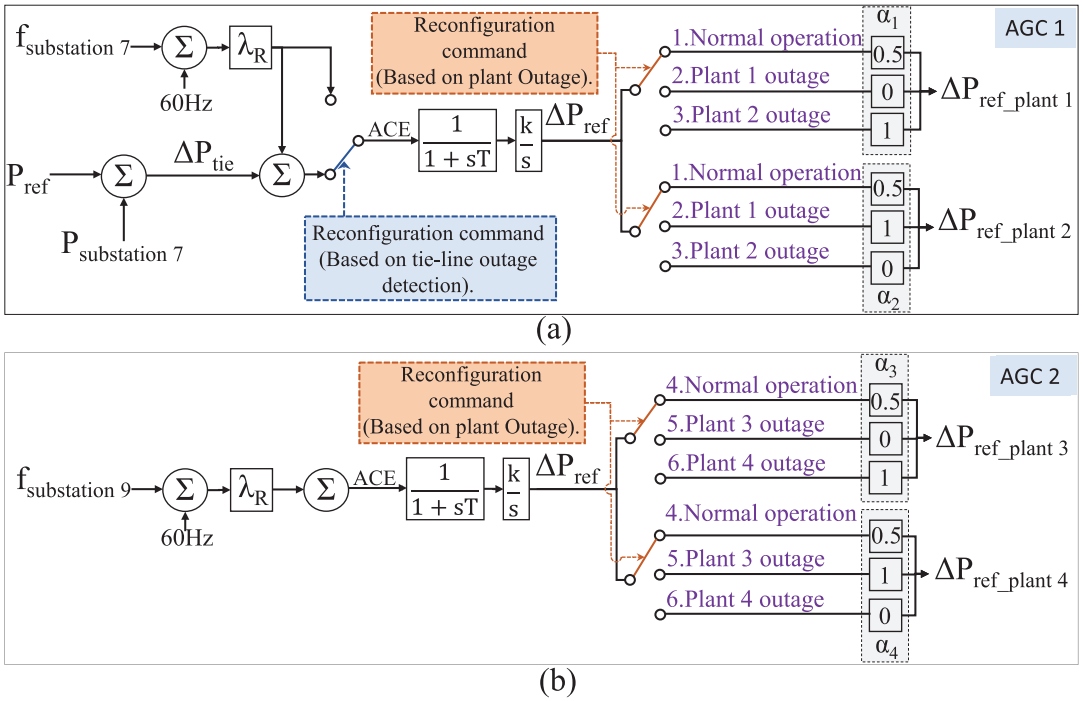

FIGURE 12. The reconfigurable AGCs block diagrams for the test system (Fig. 3). (a) Area 1 AGC and (b) Area 2 AGC.

latency for detecting and identifying the outage and initiating the reconfiguration trigger signal based on the updated TNTP. Scenario 1 (in Fig. 2) occurred in all 50 trials. However, there is a limited possibility of Scenario 2's occurrence. Therefore, a hybrid TNTP approach based on TNTP-SMRS and H-TNTP-PMUs is ideal.

The impact of AGC reconfiguration is evaluated based on the transient energy in the power flow (TEP) [35]. TEP is calculated over one minute (time difference between *tstart* & and *tstop*) using (5) where P_{Line} is the measured power flow on a transmission line (tie-lines (TL78-1 and TL78-2) or line from a power plant bus). TEP for the two case studies with TNTP-SMRS (M1) and H-TNTP-PMU (M2) is shown in Table 5. The use of LDM or NN algorithm for the H-TNTP-PMU approach does not change the TEP calculations since their computational latency (T_{CP1}) is insignificant compared to the *Total time*. For the two types of case studies investigated for AGC reconfiguration, the TEP is estimated under three

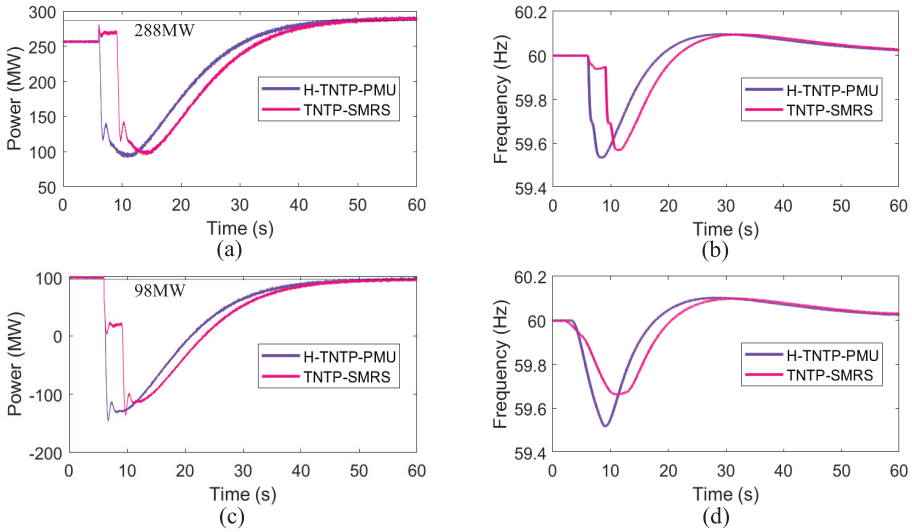

FIGURE 13. Results for power Plant 1 outage (P1O) in the test system (Fig. 3). (a) Power variations of Plant 2 (at Substation 6G) under Low operating condition, (b) Frequency variations at Substation 6G under Low operating condition, (c) Power variations of tie-line flow (at Substation 7) under High operating condition, (d) Frequency variations at Substation 7 under High operating condition.

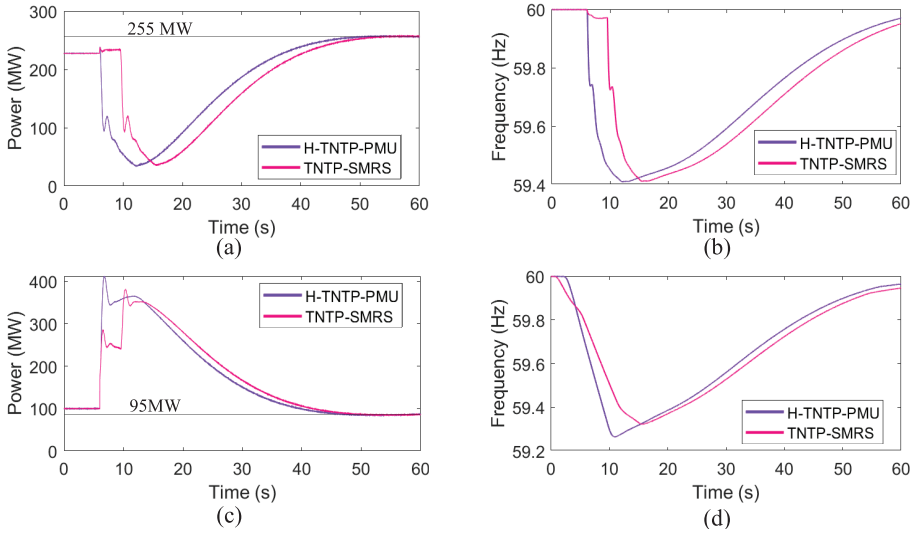

FIGURE 14. Results for power Plant 3 outage (P3O) in the test system (Fig. 3). (a) Power variations of Plant 4 (at Substation 10G) under Low operating condition, (b) Frequency variations at Substation 10G under Low operating condition, (c) Power variations of tie-line flow (at Substation 7) under High operating condition, (d) Frequency variations at Substation 7 under High operating condition.

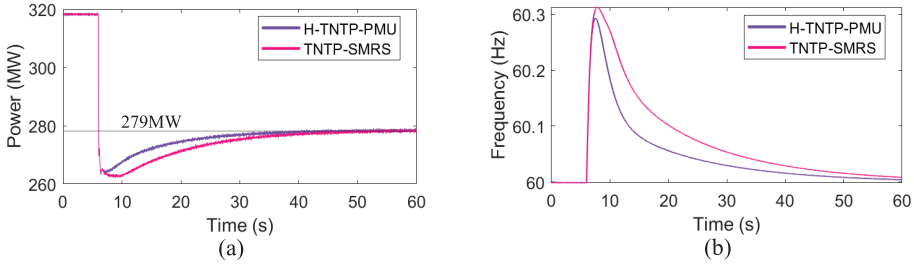

FIGURE 15. Results for area separation (tie-lines outage) (AS) in the test system (Fig. 3). (a) Power variations of Plant 2 (at Substation 6G) under High operating condition, (b) Frequency variations at Substation 6G under High operating condition.

TABLE 5. Transient energy of power flow evaluation of Plant 1 outage, Plant 3 outage, and area separation.

Case study	Operating condition	Transient energy measurement of *Line*	Transient Energy in the power flow (MWh)		
			M1	M2	Difference (M1-M2)
P1O	Low	TL6G6 (Plant 2)	55.64	55.33	0.31
		TL78-1+TL78-2	53.59	53.41	0.18
	Medium	TL6G6 (Plant 2)	70.27	70.16	0.11
		TL78-1+TL78-2	57.65	57.52	0.13
	High	TL6G6 (Plant 2)	69.62	69.47	0.15
		TL78-1+TL78-2	57.55	57.40	0.15
P3O	Low	TL10G10 (Plant 4)	74.89	74.21	0.68
		TL78-1+TL78-2	74.83	74.16	0.67
	Medium	TL10G10 (Plant 4)	88.30	87.56	0.74
		TL78-1+TL78-2	78.14	77.69	0.45
	High	TL10G10 (Plant 4)	108.54	106.71	1.83
		TL78-1+TL78-2	84.82	84.56	0.26
AS	Low	TL5G5 (Plant1)	6.00	5.97	0.03
		TL6G6 (Plant 2)	9.37	8.97	0.40
	Medium	TL5G5 (Plant1)	9.06	7.72	1.34
		TL6G6 (Plant 2)	7.93	6.46	1.47
	High	TL5G5 (Plant1)	9.01	7.67	1.34
		TL6G6 (Plant 2)	7.91	6.46	1.45

TABLE 6. Test system (Fig. 3) operating conditions for AGC reconfiguration experiments.

Operating Condition			Low		Medium		High	
			P (MW)	Q (MVAR)	P (MW)	Q (MVAR)	P (MW)	Q (MVAR)
Generation	Area 1 Plant	1	35	10	120	10	120	10
		2	255	90	320	90	320	90
		5	160	40	160	40	160	40
	Area 2 Plant	3	15	5	105	10	220	5
		4	220	70	280	70	365	60
		6	165	40	165	40	165	40
Tie-Line flow			100	-	100	-	100	-
Load	Area 1	L5	200	20	250	25	250	25
		L6	100	10	150	15	150	15
		L7	50	5	100	10	100	10
	Area 2	L9	100	10	150	15	200	20
		L10-1	100	10	150	15	200	20
		L10-2	100	10	150	15	200	20
		L11	200	20	200	20	250	25

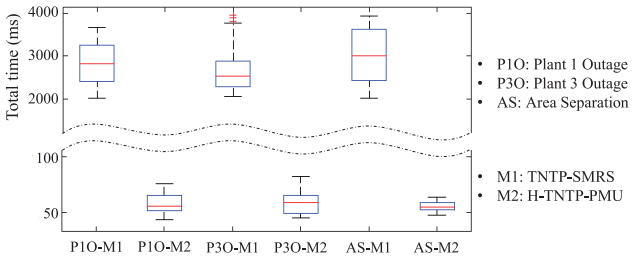

FIGURE 16. Total time to reconfigure AGCs from event initiation by H-TNTP-PMU with LDM and TNTP-SMRS.

operating conditions as shown in Table 6. It can be seen from Table 5 and Figs. 13 - 15 that AGC reconfiguration based on the H-TNTP-PMU improves the frequency regulation. This is due to the much smaller time taken by the H-TNTP-PMU approach to generate the AGC reconfiguration trigger signal.

$$TEP_{Line} = \int_{tstart}^{tstop} (P_{Line}(tstop) - P_{Line}(t))dt \qquad (5)$$

VI. CONCLUSION

Modern power system transmission network topology processing needs to be efficient and reliable in order to handle the added complexity of grid modernization. A literature review on TNTP, identifying shortcomings of the SOTA and new approaches proposed by researchers, has been presented in this paper. A physics-based hierarchical transmission

network topology processing approach, including substation configuration identification, has been presented based on node voltage and branch current measurements. The reliability and surety of the TNTP are ensured by design due to: 1) inherent verification integrated in the H-TNTP approach, 2) the ability to identify false manual switch operations due to human errors, and 3) being fault tolerant to any breaker, manual switch, or relay malfunction. The H-TNTP approach can be concurrently implemented with existing TNTP-SMRS at energy control centers, providing redundancy to energy management systems. The H-TNTP has been demonstrated on a power system with different substation arrangements and photovoltaic plants implemented on a real-time power system simulator. Furthermore, the H-TNTP using synchrophasor measurements has been implemented for fast AGC reconfiguration, and typical results have been presented illustrating better frequency regulation. Future work includes investigating the H-TNTP approach with optimal placement of PMUs and integration with advanced state estimation methods.

REFERENCES

[1] J. C. Tan, P. A. Crossley, D. Kirschen, J. Goody, and J. A. Downes, "An expert system for the back-up protection of a transmission network," *IEEE Trans. Power Del.*, vol. 15, no. 2, pp. 508–514, Apr. 2000.
[2] R. Xu, R. Wang, Z. Guan, L. Wu, J. Wu, and X. Du, "Achieving efficient detection against false data injection attacks in smart grid," *IEEE Access*, vol. 5, pp. 13787–13798, 2017.
[3] Y. Li and Y. Wang, "False data injection attacks with incomplete network topology information in smart grid," *IEEE Access*, vol. 7, pp. 3656–3664, 2019.
[4] Y. Ji, R. J. Thomas, and L. Tong, "Probabilistic forecasting of real-time LMP and network congestion," *IEEE Trans. Power Syst.*, vol. 32, no. 2, pp. 831–841, Mar. 2017.
[5] D.-H. Choi and L. Xie, "Impact of power system network topology errors on real-time locational marginal price," *J. Modern Power Syst. Clean Energy*, vol. 5, no. 5, pp. 797–809, Sep. 2017.
[6] E. A. Adel, M. Y. Sayed, and N. A. E. Amer, "IEC 61850 communication protocol with the protection and control numerical relays for optimum substation automation system," *J. Eng. Sci. Technol. Rev.*, vol. 13, no. 2, pp. 1–12, Apr. 2020.
[7] M. Farrokhabadi and L. Vanfretti, "State-of-the-art of topology processors for EMS and PMU applications and their limitations," in *Proc. 38th Annu. Conf. IEEE Ind. Electron. Soc. (IECON)*, Montreal, QC, Canada, Oct. 2012, pp. 1422–1427.
[8] X. Kong, Y. Chen, T. Xu, C. Wang, C. Yong, P. Li, and L. Yu, "A hybrid state estimator based on SCADA and PMU measurements for medium voltage distribution system," *Appl. Sci.*, vol. 8, no. 9, p. 1527, Sep. 2018. [Online]. Available: https://www.mdpi.com/2076-3417/8/9/1527
[9] S. Grijalva, "Direct utilization of planning applications in the real-time environment," in *Proc. IEEE/PES Transmiss. Distribution Conf. Expo.*, Chicago, IL, USA, Apr. 2008, pp. 1–6.
[10] NERC. *Node-Breaker Modeling Representation*. Accessed: Apr. 2, 2023. [Online]. Available: https://www.nerc.com/comm/PC/Model%20Validation%20Working%20Group%20MVWG%202013/December%202016%20-%20Node%20Breaker%20Model%20Representation%20Webinar.pdf
[11] G. Liu, C. Yuan, X. Chen, J. Wu, R. Dai, and Z. Wang, "A high-performance energy management system based on evolving graph," *IEEE Trans. Circuits Syst. II, Exp. Briefs*, vol. 67, no. 2, pp. 350–354, Feb. 2020.
[12] A. V. Ramesh, X. Li, and K. W. Hedman, "An accelerated-decomposition approach for security-constrained unit commitment with corrective network reconfiguration," *IEEE Trans. Power Syst.*, vol. 37, no. 2, pp. 887–900, Mar. 2022.
[13] L. Xu, K. Tomsovic, and A. Bose, "Topology error identification using a two-stage DC state estimator," *Electr. Power Syst. Res.*, vol. 74, no. 1, pp. 167–175, Apr. 2005.
[14] J. Liang, G. K. Venayagamoorthy, and R. G. Harley, "Wide-area measurement based dynamic stochastic optimal power flow control for smart grids with high variability and uncertainty," *IEEE Trans. Smart Grid*, vol. 3, no. 1, pp. 59–69, Mar. 2012.
[15] Z. Mirar and A. Hellal, "The role and implementation of topology processor in energy management system," in *Proc. 8th Int. Conf. Model., Identificat. Control (ICMIC)*, Nov. 2016, pp. 578–582.
[16] E. M. Lourenco, A. SimoesCosta, and K. A. Clements, "Bayesian-based hypothesis testing for topology error identification in generalized state estimation," *IEEE Trans. Power Syst.*, vol. 19, no. 2, pp. 1206–1215, May 2004.
[17] D. Singh, J. P. Pandey, and D. S. Chauhan, "Topology identification, bad data processing, and state estimation using fuzzy pattern matching," *IEEE Trans. Power Syst.*, vol. 20, no. 3, pp. 1570–1579, Aug. 2005.
[18] G. N. Korres, P. J. Katsikas, and G. E. Chatzarakis, "Substation topology identification in generalized state estimation," *Int. J. Electr. Power Energy Syst.*, vol. 28, no. 3, pp. 195–206, Mar. 2006.
[19] M. Kezunovic, "Monitoring of power system topology in real-time," in *Proc. 39th Annu. Hawaii Int. Conf. Syst. Sci. (HICSS)*, Kauia, HI, USA, 2006, pp. 1–10.
[20] C. Qian, Z. Wang, and J. Zhang, "A new algorithm of topology analysis based on PMU information," in *Proc. 5th Int. Conf. Crit. Infrastructure (CRIS)*, Sep. 2010, pp. 1–5.
[21] Y. Pradeep, P. Seshuraju, S. A. Khaparde, and R. K. Joshi, "CIM-based connectivity model for bus-branch topology extraction and exchange," *IEEE Trans. Smart Grid*, vol. 2, no. 2, pp. 244–253, Jun. 2011.
[22] K. D. Jones, J. S. Thorp, and R. M. Gardner, "Three-phase linear state estimation using phasor measurements," in *Proc. IEEE Power Energy Soc. Gen. Meeting*, Vancouver, BC, Canada, Jul. 2013, pp. 1–5.
[23] M. Farrokhabadi and L. Vanfretti, "An efficient automated topology processor for state estimation of power transmission networks," *Electr. Power Syst. Res.*, vol. 106, pp. 188–202, Jan. 2014.
[24] S. V. Wiel, R. Bent, E. Casleton, and E. Lawrence, "Identification of topology changes in power grids using phasor measurements," *Appl. Stochastic Models Bus. Ind.*, vol. 30, no. 6, pp. 740–752, Nov. 2014. [Online]. Available: https://onlinelibrary.wiley.com/doi/abs/10
[25] T. Sairam and K. S. Swarup, "Analysis of network topology processor algorithms in substation level networks," in *Proc. 7th Int. Conf. Power Syst. (ICPS)*, Dec. 2017, pp. 601–606.
[26] B. Park and C. L. Demarco, "Optimal network topology for node-breaker representations with AC power flow constraints," *IEEE Access*, vol. 8, pp. 64347–64355, 2020.
[27] C. Wang, J. An, and G. Mu, "Power system network topology identification based on knowledge graph and graph neural network," *Frontiers Energy Res.*, vol. 8, pp. 1–12, Feb. 2021, Art. no. 613331. [Online]. Available: https://www.frontiersin.org/articles/10.3389/fenrg.2020.613331
[28] A. Srivastava, S. Chakrabarti, J. Soares, and S. N. Singh, "An optimization-based topology error detection method for power system state estimation," *Electr. Power Syst. Res.*, vol. 209, Aug. 2022, Art. no. 107914. [Online]. Available: https://www.sciencedirect.com/science/article/pii/S0378779622001444
[29] J. D. McDonald, *Electric Power Substations Engineering*, 3rd ed. Boca Raton, FL, USA: CRC Press, 2012.
[30] RTDS Technologies. *Real-Time Digital Power System Simulation*. Accessed: Jan. 7, 2023. [Online]. Available: https://www.rtds.com
[31] S. S. Haykin, *Neural Networks and Learning Machines*, 3rd ed. Hoboken, NJ, USA: Prentice-Hall, 2009.
[32] D. Madurasinghe and G. K. Venayagamoorthy, "Identification of substation configurations in modern power systems using artificial intelligence," in *Proc. 11th Bulk Power Syst. Dyn. Control Symp. (IREP)*, Banff, AB, Canada, 2022, pp. 1–9.
[33] X. Li and K. W. Hedman, "Enhanced energy management system with corrective transmission switching strategy—Part I: Methodology," *IEEE Trans. Power Syst.*, vol. 34, no. 6, pp. 4490–4502, Nov. 2019.
[34] I. Jayawardene, G. K. Venayagamoorthy, and X. Zhong, "Resilient and sustainable tie-line bias control for a power system in uncertain environments," *IEEE Trans. Emerg. Topics Comput. Intell.*, vol. 6, no. 1, pp. 205–219, Feb. 2022.
[35] A. Arzani and G. K. Venayagamoorthy, "Computational approach to enhance performance of photovoltaic system inverters interfaced to utility grids," *IET Renew. Power Gener.*, vol. 12, no. 1, pp. 112–124, Jan. 2018.

DULIP MADURASINGHE (Graduate Student Member, IEEE) received the B.Sc. degree (Hons.) in electrical engineering from the University of Moratuwa, Sri Lanka, in 2017. He is currently pursuing the Ph.D. degree in electrical engineering with Clemson University, Clemson, SC, USA. He was an Embedded Engineer with Atlas Labs (Pty) Ltd., from 2017 to 2018. Currently, he is a Research Assistant with the Real-Time Power and Intelligent Laboratory, Clemson University. His current research interests include real-time power systems control and operation utilizing artificial intelligence toward resiliency.

GANESH KUMAR VENAYAGAMOORTHY (Fellow, IEEE) received the B.Eng. degree (Hons.) in electrical and electronics engineering from Abubakar Tafawa Balewa University, Bauchi, Nigeria, in March 1994, the M.Sc. (Eng.) and Ph.D. degrees in electrical engineering from the University of Natal, Durban, South Africa, in April 1999 and April 2002, respectively, and the M.B.A. degree in entrepreneurship and innovation from Clemson University, Clemson, SC, USA, in August 2016.

From 1996 to 2002, he was a Senior Lecturer with the Department of Electronic Engineering, Durban University of Technology, Durban. From 2002 to 2011, he was a Professor of electrical and computer engineering with the Missouri University of Science and Technology (Missouri S&T), Rolla, MO, USA. Since January 2012, he has been a Duke Energy Distinguished Professor of power engineering and a Professor of electrical and computer engineering with Clemson University. He is currently the Founder and the Director of the Real-Time Power and Intelligent Systems Laboratory. He led the Brain2Grid Project funded by the U.S. National Science Foundation (NSF). He is an inventor of technologies for scalable and efficient computational methods for complex systems and dynamic stochastic optimal power flow. He has published more than 600 refereed technical articles which are cited over 23,000 times with an H-index of 70 and I10-index of more than 300. He has given more than 500 invited technical presentations, including keynotes and plenaries in more than 40 countries to date. His current research interests include the research, development, and innovation of power systems, smart grids, and artificial intelligence (AI) technologies. He is a fellow of the Institution of Engineering and Technology, U.K., the South African Institute of Electrical Engineers (SAIEE), and the Asia–Pacific Artificial Intelligence Association; and a Senior Member of the International Neural Network Society (INNS). He received the 2004 US NSF CAREER Award, the 2007 U.S. Office of the Naval Research (ONR) Young Investigator Program (YIP) Award, and the 2008 NSF Emerging Frontiers in Research and Innovation (EFRI) Award. He has received several awards for faculty, research, and teaching excellence from universities, professional societies, and organizations. According to an Elsevier BV/Stanford Study, he is among the top 30,000 scientists worldwide across all fields and in the top 0.1% worldwide in the fields of energy and AI, from 2019 to 2022. He has been involved in the leadership and organization of conferences, including the Clemson University Power System Conference and a Pioneer and the Chair/Co-Chair of the IEEE Symposium of Computational Intelligence Applications in Smart Grid (CIASG), since 2011. He is also the Chair of the IEEE PES Working Group on Intelligent Control Systems and the Intelligent Systems Subcommittee and the Founder and the Chair of the IEEE Computational Intelligence Society (CIS) Task Force on Smart Grid. He has served/serves as an editor/associate editor/guest editor of several IEEE TRANSACTIONS and Elsevier journals. He is an Editor of *IEEE Press Series on Power and Energy Systems*. He is an IEEE Distinguished Lecturer of CIS, the Industry Applications Society, and the Industrial Electronics Society. He is the Vice-President of Industry Relations and a member of the Board of Governors of the International Neural Network Society.